Sensitivity curves for spaceborne gravitational wave interferometers

Shane L. Larson* and William A. Hiscock†
Department of Physics, Montana State University, Bozeman, Montana 59717

Ronald W. Hellings‡
Jet Propulsion Laboratory, Pasadena, California 91103

(Received 24 September 1999; revised manuscript received 20 March 2000; published 1 August 2000)

To determine whether particular sources of gravitational radiation will be detectable by a specific gravitational wave detector, it is necessary to know the sensitivity limits of the instrument. These instrumental sensitivities are often depicted (after averaging over source position and polarization) by graphing the minimal values of the gravitational wave amplitude detectable by the instrument versus the frequency of the gravitational wave. This paper describes in detail how to compute such a sensitivity curve given a set of specifications for a spaceborne laser interferometer gravitational wave observatory. Minor errors in the prior literature are corrected, and the first (mostly) analytic calculation of the gravitational wave transfer function is presented. Example sensitivity curve calculations are presented for the proposed LISA interferometer.

PACS number(s): 04.80.Nn, 95.55.Ym

I. INTRODUCTION

Advances in modern technology have ushered in an era of large laser interferometers designed to be used in the detection of gravitational radiation, both on the ground and in space. Such projects include the Laser Interferometric Gravitational Wave Observatory (LIGO) and VIRGO [1,2] ground-based interferometers, and the proposed Laser Interferometer Space Antenna (LISA) and OMEGA [3,4] space-based interferometers. As these detectors come on-line, a new branch of astronomy will be created and a radically new view of the Universe is expected to be revealed. With the era of gravitational wave astronomy on the horizon, much effort has been devoted to the problem of categorizing sources of gravitational radiation, and extensive studies are underway to determine what sources will be visible to the various detectors.

Typically, the sensitivity of detectors to sources of gravitational radiation has been illustrated using graphs which compare source strengths (dimensionless strain) to instrument noise as functions of the gravitational wave frequency. Many different types of plots have appeared in the literature, ranging from single plots of spectral density to separate amplitude plots for each class of source. When considering the possibility of observing a new source, or comparing aspects of various proposed gravitational wave observatories, it is important to be able to generate consistent and accurate noise curves for a given instrument and to understand what assumptions have gone into generating the curves. This is especially important in the case of spaceborne gravitational observatories which are sensitive to low frequency (LF) gravitational waves (in the band from 10^{-4} Hz to 1 Hz). In this LF band, the sources of radiation include both *known* continuous sources at well-determined strengths and frequencies [5], for which a signal-to-noise ratio only slightly greater than one is needed for detection, as well as speculative short-lived ''burst'' sources requiring a much greater signal-to-noise ratio for detection.

This paper reviews the mathematical formalism and methodology for generating noise curves for a class of spaceborne gravitational wave interferometers. A synthesis is provided here of material which has hitherto been scattered across the literature, and a variety of new results are incorporated. The gravitational wave transfer function of an interferometer, averaged over source direction and polarization, is calculated here for the first time,[1] and a number of minor errors in the existing literature are corrected. Although the results of this paper are applicable to any spaceborne laser interferometer system designed for gravitational wave detection, specifics of the proposed LISA mission are used as an example.

The outline of the paper is as follows. In Sec. II, the concept of instrumental operation for a spaceborne interferometer is described. Section III discusses noise sources that limit the sensitivity of the detector and Sec. IV presents the mathematical formalism for generating sensitivity curves from these noise sources. Section V considers the various types of sensitivity curves which currently exist in the literature and reconciles the different methods.

II. INSTRUMENT OPERATION

A. Instrument design

The common design concept for proposed spaceborne interferometers consists of a constellation of probes arranged

*Electronic mail address: shane@physics.montana.edu
†Electronic mail address: hiscock@montana.edu
‡Electronic mail address: hellings@graviton.jpl.nasa.gov

[1]While this paper was in preparation, we became of aware of recent work by Armstrong, Estabrook, and Tinto [6] which numerically estimates the gravitational wave transfer function using Monte Carlo simulations to conduct the averaging. A visual inspection of the sensitivity curve derived from the transfer function derived by [6] shows agreement with the results derived in this paper.

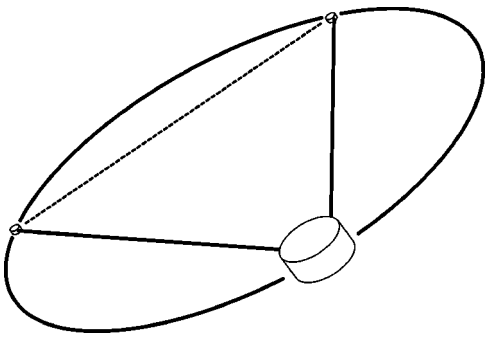

FIG. 1. A typical configuration for a spaceborne gravitational wave interferometer. Three probes form an equilateral triangle, inscribed on the relative orbits of the spacecraft. A single Michelson interferometer is formed using any two legs of the triangle, and a second (non-independent) interferometer can be formed using the third arm of the configuration in conjunction with an arm already in use for the primary signal.

in an equilateral triangle inscribed on the circle of the probes' relative orbits. In the simplest configuration, 3 probes are used to form a single Michelson interferometer, as shown in Fig. 1. The probe at the vertex of the angle corresponds to the central mirror in the interferometer, while the two probes on the ends of the arms correspond to the end mirrors. The effect of a gravitational wave passing by the detector is to stretch or contract space in the arms of the interferometer. The effects in the two arms will in general be different, due to the different orientation of the two arms in space. The wave is detected by monitoring the times of flight of laser signals between the probes in order to observe and measure this difference. The basic operation of a space gravitational wave detector consists in measuring the phases of the incoming laser signals relative to those of the outgoing signals in both arms of the interferometer and differencing these relative phases to cancel common phase noise in the two arms.

In order to avoid spurious motions of the spacecraft that could mimic the effect of a gravitational wave on the laser tracking signals, each spacecraft is equipped with a position control system. This system consists of, first, an accelerometer that measures the motion of the spacecraft relative to a proof mass that floats freely at the center of the accelerometer and, second, a set of thrusters that accelerate the spacecraft. A control loop fires the thrusters in such a way as to null the output from the accelerometer and maintain the spacecraft on a purely gravitational trajectory.

B. Gravitational wave response

The response of an electromagnetic tracking signal to the passage of a gravitational wave has been shown by Estabrook and Wahlquist [9] to be a Doppler shift in the frequency of the received signal relative to the outgoing signal. For a gravitational wave of amplitude $h(t)$, the shift in a signal of fundamental frequency ν_o will be given by

$$\frac{\Delta\nu(t,\theta,\psi)}{\nu_o}=\frac{1}{2}\cos 2\psi[(1-\cos\theta)h(t)+2\ \cos\ \theta \times h(t-\tau-\tau\cos\theta)-(1+\cos\theta)h(t-2\tau)], \tag{1}$$

where τ is the light travel time between end masses, θ is the angle between the lines-of-sight to the probe and to the source, and ψ is a principal polarization angle of the quadrupole gravitational wave.

The angles θ and ψ will, for a general spaceborne interferometer, be slowly varying functions of time, dependent upon the orbital configuration of the detector. This paper ignores these time dependencies, which are specific to a particular mission design, so that the only time dependence assumed in Eq. (1) is the time varying amplitude of the gravitational wave, $h(t)$. The sky-averaged sensitivity obtained by averaging over the antenna pattern associated with a particular interferometer orbital configuration will be negligibly different from the all-sky average obtained here for a fictitious spatially fixed interferometer.[2]

It is useful to write $h(t)$ in terms of its Fourier transform $\tilde{h}(\omega)$. If the Doppler record is sampled for a time T then $h(t)$ is related to its Fourier transform by

$$h(t)=\frac{\sqrt{T}}{2\pi}\int_{-\infty}^{+\infty}\tilde{h}(\omega)e^{i\omega t}d\omega, \tag{2}$$

where the $\sqrt{T}$ normalization factor is used to keep the power spectrum roughly independent of time. Using this definition of the Fourier transform and Eq. (1), the frequency shift can be written as

$$\Delta\nu(t,\theta,\psi)=\nu_o\frac{\sqrt{T}}{2\pi}\int_{-\infty}^{+\infty}\frac{1}{2}\cos(2\psi)\tilde{h}(\omega,\theta,\psi)[(1-\mu)+2\mu e^{-i\omega\tau(1+\mu)}-(1+\mu)e^{-i2\omega\tau}]e^{i\omega t}d\omega, \tag{3}$$

where $\mu\equiv\cos\theta$. The quantity that is actually read out by the laser interferometer tracking system is phase, so Eq. (3) is integrated to find the phase in cycles

$$\Delta\phi(t,\theta,\psi)=\int_0^t\Delta\nu(t',\theta,\psi)dt'. \tag{4}$$

If the phase is divided by the laser frequency and the one-way light travel time of each arm, one obtains

[2]The angles θ and ψ will vary at the orbital period of the interferometer, T_{orb}. In calculating the response to a gravitational wave of period T_{gw}, the relative error in the power spectrum made by assuming the angles to be constant will be of order $(T_{gw}/T_{orb})^2$. As long as the orbital period is much longer than the gravitational wave period, this error will be negligible.

$$z(t,\theta,\psi)=\frac{\Delta\phi(t,\theta,\psi)}{\nu_o\tau}$$
$$=\frac{\sqrt{T}}{4\pi\tau}\int_{-\infty}^{+\infty}d\omega\cos(2\psi)\tilde{h}(\omega)[(1-\mu)$$
$$+2\mu e^{-i\omega\tau(1+\mu)}-(1+\mu)e^{-i2\omega\tau}]\frac{1}{i\omega}e^{i\omega t}, \tag{5}$$

where Eq. (3) has been used to expand $\Delta\nu(t,\theta,\psi)$, and arbitrary constant phases have been set to zero in the integration of Eq. (4). The $1/\omega$ in the Fourier integral arises from the integration in the time domain in Eq. (4). This $z(t,\theta,\psi)$ has the property that, in the limit of low frequency, it reduces to a pure spatial strain. At high frequencies, the signal is much more complicated due to the three h-terms that enter at different times. Nevertheless, in what follows we will loosely refer to the quantity $z(t,\theta,\psi)$ as the gravitational wave strain.

The goal of gravitational wave detection is to detect the strain produced by a gravitational wave signal, as given in Eq. (5), in the presence of competing noise. The primary sources and spectra of this noise will be discussed in the next section.

III. NOISE SPECTRA

A. Common noise spectra

The signal received in a single arm of the interferometer is given by

$$s_i(t)=z(t,\theta_i,\psi_i)+p(t)-p(t-2\tau_i)+n_i(t), \tag{6}$$

where $s_1(t)$ and $s_2(t)$ are the two noisy strain signals in the two arms of the interferometer, $p(t)$ is the laser phase noise which is common to the two arms, $n_i(t)$ is the strain noise in the i^{th} arm produced by all other noise sources, and τ_i is the one-way light travel time in the i^{th} arm. The major source of noise in each arm, by several orders of magnitude, is the $p(t)$ phase noise in the lasers. However, this noise is common to both arms of the interferometer and can be eliminated through signal processing. When an interferometer signal

$$\Sigma(t)=s_1(t)-s_2(t)$$
$$=z_1(t)-z_2(t)+n_1(t)-n_2(t)-p(t-2\tau_1)+p(t-2\tau_2) \tag{7}$$

is formed, the laser phase noise will cancel as $\tau_1\rightarrow\tau_2$. Unfortunately, a space-based interferometer consisting of freely flying spacecraft will necessarily have unequal armlengths, preventing effective use of $\Sigma(t)$ as a signal for data analysis.

However, a new data reduction procedure for space interferometry has been recently discovered and discussed in a paper by Tinto and Armstrong [10]. This method eliminates all laser phase noise even if the two light travel times τ_1 and τ_2 are unequal. Working in the time domain, one defines the combination

$$X(t)=s_1(t)-s_2(t)-s_1(t-2\tau_2)+s_2(t-2\tau_1)$$
$$=z_1(t)-z_2(t)-z_1(t-2\tau_2)+z_2(t-2\tau_1)$$
$$+n_1(t)-n_1(t-2\tau_2)-n_2(t)+n_2(t-2\tau_1), \tag{8}$$

which is devoid of laser phase noise for all values of the two light travel times τ_1 and τ_2. In order for the laser phase noise to cancel exactly, both light travel times must be known exactly so that the combination of signals in Eq. (8) can be correctly formed. In practice, however, all that is necessary is for the armlengths to be known well enough for the laser phase noise to become insignificant relative to the independent noise sources (discussed next).

B. Independent noise spectra

Since noise common to the two arms of an interferometer can be significantly reduced by the procedure just described, the limiting sensitivity of the space-based gravitational wave missions is actually determined by noise sources that are independent in the two arms of the interferometer. The quantity that needs to be calculated for each such noise source is the phase noise the source produces in a round-trip signal. This will produce strain noise $n(t)$ to compete with the gravitational wave signal $z(t)$ [see Eq. (6)]. From Eq. (5), the relation between the spectral density of strain noise and the spectral density of phase noise is seen to be

$$S_n=\frac{S_\phi}{\nu_0^2\tau^2}. \tag{9}$$

In Eq. (9), S_ϕ is assumed to represent the total noise contribution of a specific type, produced in the one-arm round-trip signal. However, each arm is composed of two spacecraft whose leading noise sources are statistically independent of each other. Redefining S_ϕ to be the noise of a particular type in each spacecraft, Eq. (9) can be rewritten

$$S_n=\frac{2S_\phi}{\nu_o^2\tau^2} \tag{10}$$

where S_ϕ is now the noise contributed by a single spacecraft.

The noise curves for space gravitational wave detectors are dominated by acceleration noise at low frequencies and by position noise at high frequencies. In what follows, we will consider some of the major sources of this noise.

The most important single source of position noise in the current designs is shot noise in the detection of the weak laser signals. Shot noise produces a phase noise (in cycles) given by

$$S_\phi=\frac{h\nu_o}{4\pi^2P_r} \tag{11}$$

where $h\nu_o$ is the photon energy and P_r is the received power. The received power is calculated from

$$P_r=P_t\left[\frac{\epsilon\pi^2\nu_o^2D^2}{c^2}\right]\left[\frac{1}{4\pi r^2}\right]\left[\frac{\epsilon\pi D^2}{4}\right] \tag{12}$$

where P_t is the transmitted power, the quantity in the first square brackets is the directional gain of the transmitter optics with diameter D and efficiency ϵ for light of frequency ν_o, the quantity in the second square brackets is the space loss at a distance r, and the quantity in the last square brackets is the effective cross section of the receiving optics. Combining Eqs. (10)–(12), the formula for the strain noise produced in each arm by laser shot noise is

$$S_n = 2\frac{4c^4}{\pi^4}\frac{h\nu_o}{\epsilon^2 D^4 P_t}\frac{1}{\nu_o^4}, \tag{13}$$

where we have used the fact that $r \approx c\tau$. The leading factor of 2 comes from Eq. (10) and accounts for the fact that there are two lasers in each arm of the interferometer (one in each spacecraft).

There are other one-way noises that affect either the incoming signal only (such as thermal noise in the receiver electronics) or the outgoing signal only (such as pointing errors that rotate the outgoing nonspherical wave front). If the effective position noise of such errors has spectral density S_x, then the phase noise they produce in the round-trip signal will have spectral density

$$S_\phi = \frac{\nu_o^2}{c^2} S_x \tag{14}$$

where S_ϕ is in cycles^2 Hz^{-1} and S_x is in m^2 Hz^{-1}. Other position noise sources, such as thermal variations in the path through one spacecraft's optics, will affect both incoming and outgoing signals and so will produce phase noise with spectral density given by

$$S_\phi = 4\frac{\nu_o^2}{c^2} S_x . \tag{15}$$

Acceleration noise acting on the proof mass in each spacecraft is a noise source of this second type, since a physical motion of the proof mass will change the path length of both incoming and outgoing signals. Acceleration noise from a single proof mass will thus produce phase noise in the received two-way signal given in cycles by

$$S_\phi(f) = 4\frac{\nu_o^2 S_a}{c^2 (2\pi f)^4} \tag{16}$$

where S_a is the acceleration spectral density in m^{2}s^{-4}Hz^{-1} and the factor of 4 comes from doubling the effect by acting on both incoming and outgoing signals. Equations (14)–(16) are the phase noises produced from position noise in a single spacecraft; the total position noise in an interferometer arm is found by using the appropriate S_ϕ in Eq. (10).

For the current LISA design, the strengths of many of these noise sources have been budgeted. The shot noise is expected to have phase spectral density $S_\phi(f) = 1.2 \times 10^{-10}$ cycles^2 Hz^{-1}, while the total one-way position noise (including shot noise) is allowed spectral density $S_x(f) = 1.6 \times 10^{-21}$ m^2 Hz^{-1} [3]. The major source of acceleration noise in the space detectors is expected to be parasitic forces acting on the proof mass of the accelerometer. Accelerometers are very complex and the noise is difficult to characterize, especially in the laboratory tests where the proof mass must be suspended in one-g rather than being allowed to float freely in space. Nevertheless, from what has been learned in the laboratory, it appears that a flat acceleration noise spectrum at a level of $S_a = 9 \times 10^{-30}$ m^2 s^{-4} Hz^{-1} should be achievable over most of the frequency band of interest (this is the level assumed in the present LISA design [3]).

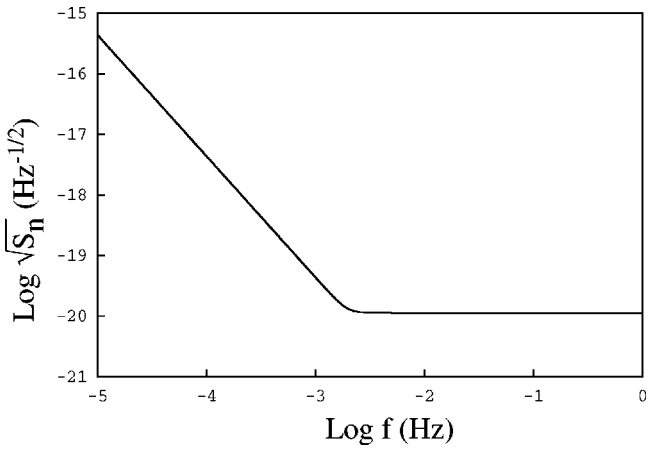

FIG. 2. The root spectral density of the noise in the LISA interferometer formed by adding the strain noises induced by acceleration noise and by total position noise in quadrature.

The total noise curves for space gravitational wave detectors are found by adding the various noise spectra in quadrature. Using the values given above for the LISA mission, this total root spectral density of the instrument is as plotted in Fig. 2.

IV. GENERATION OF SENSITIVITY CURVES

The sensitivity of an instrument to a gravitational wave depends on the relationship between the amplitude of the wave and the size of the signal that eventually appears in the detector. It also depends on the size of the noise in the final output signal of the instrument. The connection between amplitude and signal is calculated in frequency space and is called the *transfer function*. If the interferometer output $\Sigma(t)$ has a gravitational wave contribution to it given by

$$\Delta(t) = z_1(t) - z_2(t), \tag{17}$$

then the transfer function $R(\omega)$ is defined by

$$S_{\bar{\Delta}}(\omega) = S_h(\omega) R(\omega), \tag{18}$$

where the gravitational wave amplitude spectral density $S_h(\omega)$ is defined by

$$S_h(\omega) = |\tilde{h}(\omega)|^2, \tag{19}$$

so that the mean-square gravitational wave strain is given by

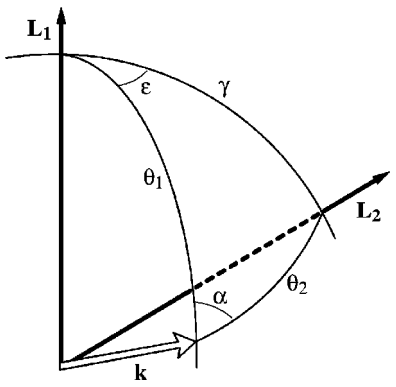

FIG. 3. The geometrical relationship of the interferometer to the propagation vector of a gravitational wave, used to conduct spatial averaging. The arms are designated by vectors $\mathbf{L}_1$ and $\mathbf{L}_2$ (solid black vectors), while the propagation vector of the gravitational wave is given by $\mathbf{k}$ (open white arrow). One arm of the interferometer is aligned along the polar axis of a 2-sphere, the other arm lying an angular distance γ away long a line of constant longitude. The angles θ_i relate the vector $\mathbf{k}$ to the arms of the interferometer, and the angle ϵ is the inclination of the plane containing $\mathbf{k}$ and $\mathbf{L}_1$ to the plane of the interferometer.

$$\langle h^2\rangle = \frac{1}{T}\int_0^\infty h(t)^2 dt = \frac{1}{2\pi}\int_0^\infty S_h(\omega)\,d\omega. \tag{20}$$

Similarly, the instrumental response $S_{\overline{\Delta}}(\omega)$ is defined such that

$$\overline{\langle \Delta^2\rangle} = \frac{1}{2\pi}\int_0^\infty S_{\overline{\Delta}}(\omega)\,d\omega, \tag{21}$$

where the brackets indicate a time average and the bar over the Δ in Eq. (21) indicates that it is averaged over source polarization and direction.

In the next section, the transfer function from the gravitational wave amplitude h to the interferometer signal $\overline{\Delta}$ (which is the signal part of Σ) is worked out. As discussed in Sec. III A, the preferred instrumental output would actually be $X(t)$, defined in Eq. (8), since it exactly cancels the laser phase noise in the data. However, $X(t)$ is a difficult quantity to work with since its transfer function will depend on the particular values of the interferometer arm lengths, τ_1 and τ_2. One approach to simplify the calculation is to assume $\tau_1 = \tau_2$. (This approach is taken in Ref. [6].) At the end of the next section, we will give the transfer function for $X(t)$ with this assumption made, and will show that in this limit $\Sigma(t)$ and $X(t)$ yield the same instrumental sensitivity.

A. Gravitational wave transfer function

Previous estimates of sensitivity [8] have often resorted to working in the long wavelength approximation, beginning from the Doppler tracking signal described by Eq. (1), or have combined results for independent single arms. Here the *exact* gravitational wave transfer function is computed, without such approximations, from the gravitational wave strain.

Consider the geometry shown in Fig. 3. The vectors $\mathbf{L}_1$ and $\mathbf{L}_2$ point along the arms of the interferometer, and the vector $\mathbf{k}$ points along the propagation vector of the gravitational wave. The quantities θ_i measure the angular separation between the arm vectors and the propagation vector. The value γ is the opening angle of the interferometer, and ϵ is the inclination of the plane containing $\mathbf{k}$ and $\mathbf{L}_1$ to the plane of the interferometer.

Not shown are the principal polarization vectors of the gravitational wave, which lie in a plane 90° away from $\mathbf{k}$. The polarization angles, ψ_i, are measured from the point where the plane of the i^{th} arm and the propagation vector intersects the plane containing the principal polarization vector. The angle α in Fig. 3 is simply the difference of the two polarization angles, $\alpha = \psi_2 - \psi_1$.

The average power in the interferometer is given by

$$\langle \Delta^2\rangle = \lim_{T\to\infty}\frac{1}{T}\int_0^\infty |\Delta|^2 dt, \tag{22}$$

where Δ is defined by Eq. (17). Using the definition of z from Eq. (5) this can be expanded to yield

$$\langle \Delta^2\rangle = \frac{1}{2\pi}\int_0^\infty d\omega \tilde{h}^2(\omega)\frac{1}{(\omega\tau)^2}[T_1(\omega)+T_2(\omega)-2T_3(\omega)], \tag{23}$$

where

$$\begin{aligned} T_1(\omega) = \cos^2(2\psi_1)[\mu_1^2(1+\cos^2(\omega\tau)) + \sin^2(\omega\tau) \\ - 2\mu_1^2\cos(\omega\tau)\cos(\omega\tau\mu_1) \\ - 2\mu_1\sin(\omega\tau)\sin(\omega\tau\mu_1)], \end{aligned} \tag{24}$$

$$\begin{aligned} T_2(\omega) = \cos^2(2\psi_2)[\mu_2^2(1+\cos^2(\omega\tau)) + \sin^2(\omega\tau) \\ - 2\mu_2^2\cos(\omega\tau)\cos(\omega\tau\mu_2) \\ - 2\mu_2\sin(\omega\tau)\sin(\omega\tau\mu_2)], \end{aligned} \tag{25}$$

$$T_3(\omega) = \cos(2\psi_1)\cos(2\psi_2)\,\eta(\omega), \tag{26}$$

with $\mu_i = \cos\theta_i$, and where

$$\begin{aligned} \eta(\omega,\theta_1,\theta_2) = [\cos(\omega\tau)-\cos(\omega\tau\mu_1)][\cos(\omega\tau) \\ - \cos(\omega\tau\mu_2)]\mu_1\mu_2 + [\sin(\omega\tau) \\ - \mu_1\sin(\omega\tau\mu_1)][\sin(\omega\tau)-\mu_2\sin(\omega\tau\mu_2)], \end{aligned} \tag{27}$$

has been defined for convenience. The expression for the power in the detector, as given by Eq. (23), is a complicated function of frequency and of the orientation between the propagation vector of the gravitational wave and the interferometer. It represents the antenna pattern for a laser interferometer gravitational wave detector. At low frequencies, the frequency dependence drops out and the expressions simplify greatly [11], but at higher frequencies it remains a very complicated frequency-dependent object.

To characterize the average sensitivity of the instrument it is customary to consider the isotropic power, obtained by averaging the antenna pattern over all propagation vectors and all polarizations:

$$\overline{\langle \Delta^2 \rangle} = \frac{1}{8\pi^2} \int_0^{2\pi} d\psi \int_0^{2\pi} d\epsilon \int_0^{\pi} \sin\theta d\theta \langle \Delta^2 \rangle. \tag{28}$$

Since the variables (θ_1, ψ_1) and (θ_2, ψ_2) that figure in Eq. (23) each locate the same propagation vector of the gravitational wave, they are not independent of one another. However, examination of Eqs. (24)–(26) shows that T_1 depends only on the (θ_1, ψ_1) variables, while T_2 depends only on (θ_2, ψ_2). This allows the integration of Eq. (28) to be performed very easily for the T_1 and T_2 terms without converting to a common set of angular variables. In each case, the averaging of the T_1 and T_2 terms over the (θ_i, ψ_i) gives precisely the same value:

$$\begin{aligned} \overline{T_1} = \overline{T_2} &= \frac{1}{8\pi^2} \int d\psi_1 \, d\epsilon \, d\theta_1 \, \sin\theta_1 \, T_1 \\ &= \frac{1}{2} \left[(1 + \cos^2(\omega\tau)) \left(\frac{1}{3} - \frac{2}{(\omega\tau)^2} \right) + \sin^2(\omega\tau) \right. \\ &\quad \left. + \frac{4}{(\omega\tau)^3} \sin(\omega\tau)\cos(\omega\tau) \right]. \end{aligned} \tag{29}$$

The average isotropic power can then be expressed as

$$\overline{\langle \Delta^2 \rangle} = \frac{1}{\pi} \int_0^{\infty} d\omega \, \tilde{h}^2(\omega) \frac{1}{(\omega\tau)^2} [\overline{T_1} - \overline{T_3}]. \tag{30}$$

To complete the integration, the function T_3 [which depends on both (θ_1, ψ_1) and (θ_2, ψ_2)] must finally be expressed in terms of a single set of angular variables. One may choose to eliminate (θ_2, ψ_2) in favor of (θ_1, ψ_1) by using conventional spherical trigonometry in Fig. 3. For the polarization angle, the relationship is particularly simple

$$\psi_2 = \psi_1 + \alpha$$

and the integration over ψ_1 may be carried out analytically, giving

$$\begin{aligned} \overline{T_3} &= \frac{1}{8\pi^2} \int d\psi_1 \, d\epsilon \, d\theta_1 \, \sin\theta_1 \, T_3 \\ &= \frac{1}{8\pi} \int d\epsilon \, d\theta_1 \, \sin\theta_1 \, \cos(2\alpha) \, \eta(\omega, \theta_1, \theta_2). \end{aligned} \tag{31}$$

The cost of carrying out the ψ_1 integration is the introduction of the angle α, which can be related to the $\{\epsilon, \theta_i\}$ variables using the law of sines in Fig. 3:

$$\sin\alpha = \frac{\sin\gamma \sin\epsilon}{\sin\theta_2}. \tag{32}$$

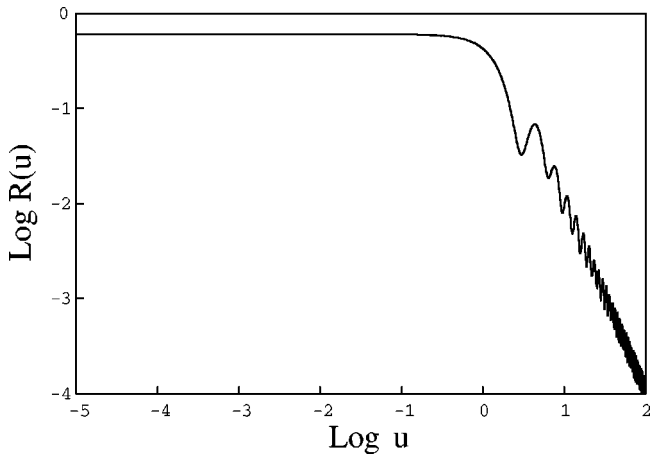

FIG. 4. The transfer function $R(u)$ is shown as a function of the dimensionless variable $u = \omega\tau$. Note that it is roughly constant at low frequencies, and has a ''knee'' located at $u = \omega\tau \sim 1$.

The function $\eta(\omega, \theta_1, \theta_2)$ in Eq. (27) has terms containing $\mu_2 = \cos\theta_2$, which must be re-expressed in terms of the integration variable θ_1. The relationship between θ_1 and θ_2 is given by

$$\cos\theta_2 = \cos\gamma\cos\theta_1 + \sin\gamma\sin\theta_1\cos\epsilon, \tag{33}$$

where γ is the opening angle of the interferometer, and ϵ is the inclination of the gravitational wave propagation vector to the interferometer. Due to the complexity of $\eta(\omega)$ when Eq. (33) is substituted into Eq. (27), we have not been able to calculate an expression for $\overline{T_3}$ analytically, so it will be kept as an explicit integral.

Using the definition of $R(\omega)$ from Eq. (18) with the average isotropic power in Eq. (30), the gravitational wave transfer function is found to be

$$\begin{aligned} R(\omega) &= 2 \frac{1}{(\omega\tau)^2} [\overline{T_1} - \overline{T_3}] \\ &= \frac{1}{(\omega\tau)^2} \left[(1 + \cos^2(\omega\tau)) \left(\frac{1}{3} - \frac{2}{(\omega\tau)^2} \right) + \sin^2(\omega\tau) \right. \\ &\quad + \frac{4}{(\omega\tau)^3} \sin(\omega\tau)\cos(\omega\tau) \\ &\quad \left. - \frac{1}{4\pi} \int d\epsilon \, d\theta_1 \, \sin\theta_1 (1 - 2\sin^2\alpha) \, \eta(\omega) \right]. \end{aligned} \tag{34}$$

It is straightforward to evaluate the remaining integral using simple numerical techniques. The exact transfer function, including the numerical evaluation of the last integral, is shown in Fig. 4 as a function of the dimensionless quantity $u = \omega\tau$.

The high frequency structure in Fig. 4 dominates the shape of the transfer function at frequencies greater than $\omega \simeq 1/\tau$. At these frequencies, the armlength τ of the interferometer becomes comparable to the wavelength of the gravi-

tational wave. The extrema in the transfer function are amplifications due to interference of the signals in the arms. The minima occur at frequencies

$$f = n/2\tau. \tag{35}$$

The appearance of these periodic amplifications is familiar from basic interferometry.

Taking the limit of small $\omega\tau$ in Eq. (34) will yield a low frequency limit for S_{Δ}^{-} of

$$S_{\Delta}^{-} = \frac{4}{5}\sin^2\gamma\, S_h, \tag{36}$$

which is in agreement with a previous result from Hellings [8].[3]

B. Sensitivity curves

The sensitivity curve for a gravitational wave observatory is obtained from Eq. (18) in the case where the spectral density of the isotropic power, S_{Δ}^{-}, is equal to the spectral density of noise in the detector. The noise in the final instrumental signal may be related to the hardware noise in each detector by inspection of Eq. (7). Assuming that $n_1(t)$ and $n_2(t)$ are uncorrelated, the spectral density of the signal produced by phase measurement noise is

$$S_N = 2S_n, \tag{37}$$

where S_n is the spectral density of noise. The factor of 2 in Eq. (37) comes from the two $n_i(t)$ in Eq. (7) adding in quadrature, since they are uncorrelated. The final equation for gravitational wave amplitude sensitivity is thus

$$S_h = \frac{S_{\Delta}^{-}}{R} = \frac{S_N}{R} = \frac{2S_n}{R}. \tag{38}$$

The spectral amplitude sensitivity is simply the square root of S_h, or

$$h_f = \sqrt{S_h} = \sqrt{2\frac{S_n}{R}}. \tag{39}$$

Using the noise curve given in Fig. 2, and using the LISA value of $c\tau = 5\times10^9$ m, the LISA sensitivity curve, computed using Eq. (39), is shown in Fig. 5. The position of the high frequency ''knee'' occurs at $f = 1/(2\pi\tau) = 10^{-2}$ Hz.

The greatest sensitivity is seen to occur in a mid-frequency ''floor;'' the level of this floor is set by the size of the position noise. The width of the floor is a function of the acceleration noise level and the arm length of the interferometer. The low frequency rise occurs when acceleration noise begins to dominate over position noise; the high frequency rise is caused by the turnover in the transfer function, at $f \simeq 1/(2\pi\tau)$.

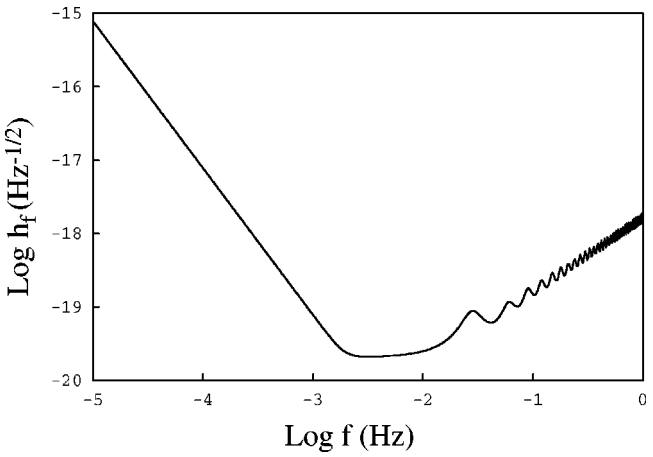

FIG. 5. The sensitivity curve for the proposed LISA observatory is shown. The low frequency rise is due to acceleration noise in the system. The high frequency rise is due to the ''knee'' in the transfer function at $f \simeq (2\pi\tau)^{-1}$. The structure at high frequencies is a consequence of the high frequency structure in the gravitational wave transfer function.

C. Comparison with prior results

One may compare the transfer function of Eq. (34) with others that have previously appeared in the literature. In general, previous results have approximated the transfer function by working in the low frequency limit, where the transfer function becomes constant [8].[4]

For the specific case of LISA, the transfer functions which have previously been published [3,7] represent a time-average over the LISA orbit and averages over azimuth and polarization, but not over source declination (separate transfer functions are shown for specific values of source declination). The work presented in this paper is more general, averaging over source declinations rather than the specific characteristics of the LISA orbit. The transfer function of Eq. (34) is the first with true all-sky averaging valid at all frequencies. Also, the previous transfer functions for LISA have been incorrectly normalized at high frequencies. The problem with these transfer functions is they have been obtained by multiplying the maximal response of the interferometer to a high-frequency source (with optimal polarization and direction) by the value of the transfer function in the low-frequency limit, as given by Eq. (36). The actual transfer function, given by Eq. (34), is much more complicated than this, as may be seen in the complicated dependence on fre-

[3]In the notation of this paper, the interferometer signal has been multiplied by the laser period and divided by the arm length of the interferometer, as described in Eq. (5). To agree with the expressions for the spectral density of the interferometer signal S_δ in the literature, this factor must be accounted for above, so that $S_\delta = (\tau\nu_o)^2 S_{\Delta}^{-}$.

[4]The full transfer function has not been needed for the ground-based interferometers such as LIGO since in their operation (as Fabry-Pérot cavities) the low frequency limit is valid up to about 40−50 kHz.

quency and interferometer opening angle γ (γ enters through the parameters η and α).

D. The transfer function for $X(t)$

As discussed at the beginning of Sec. IV, the preferred signal from the interferometer for purposes of data analysis is not $\Sigma(t)$, but $X(t)$, since the common laser phase noise exactly cancels in $X(t)$. Unfortunately, the transfer function for $X(t)$ depends in a complicated way on the particular values of τ_1 and τ_2. However, substantial simplification occurs in the special case $\tau_1 \approx \tau_2 = \tau$, which was treated in Ref. [6]. In this case, the formula for $X(t)$ becomes

$$X(t) = z_1(t) - z_2(t) - [z_1(t-2\tau) - z_2(t-2\tau)] + n_1(t) - n_2(t) - [n_1(t-2\tau) - n_2(t-2\tau)], \tag{40}$$

which may also be written as

$$X(t) = \Xi(t) + \sigma(t) \tag{41}$$

where

$$\Xi(t) = \Delta(t) - \Delta(t-2\tau), \tag{42}$$

and

$$\sigma(t) = N(t) - N(t-2\tau). \tag{43}$$

Here $\Delta(t)$ is given by Eq. (17) and $N(t) \equiv n_1(t) - n_2(t)$.

The portion of $X(t)$ which is a gravitational wave signal is then, by Eq.(42), simply two copies of the Δ signal we have previously analyzed. The transfer function for $\Xi(t)$ may be calculated following the procedure in Sec. IV A, to find

$$S_\Xi(\omega) = 4\sin^2(\omega\tau) S_{\bar{\Delta}}(\omega) = 4\sin^2(\omega\tau) S_h(\omega) R(\omega), \tag{44}$$

where Eq. (18) has been used for the second equality. The transfer function for X will then be

$$R_X(\omega) = 4\sin^2(\omega\tau) R(\omega), \tag{45}$$

where $R(\omega)$ is the previously derived transfer function for Δ, given by Eq. (34).

At first glance, it appears the that transfer function for X could be as large as four times the transfer function for Δ, and hence that weaker gravitational waves could be observed by constructing X. However, to determine the sensitivity of the interferometer, one must equate $S_\Xi(\omega)$ in Eq. (44) to the appropriate spectral density of noise. For X, this is formed using the $\sigma(t)$ combination defined in Eq. (43). Because the noise contribution to X is formed by the same subtraction process, it will similarly have

$$S_\sigma(\omega) = 4\sin^2(\omega\tau) S_N(\omega). \tag{46}$$

The additional factors due to the subtraction process used to form X, which appear in Eqs. (44),(46), will cancel in the computation of the sensitivity limit of the interferometer:

$$S_h = \frac{S_\sigma}{R_X} = \frac{4\sin^2(\omega\tau) S_N(\omega)}{R_X} = \frac{2S_n}{R}, \tag{47}$$

where the second equality follows from Eq. (45) and the definition of N in terms of the n_i.

Thus, in the limit as $\tau_1 \to \tau_2$, the sensitivity curve for $X(t)$ will be identical to that previously computed for $\Delta(t)$, as shown in Fig. 5. We are investigating transfer functions for unequal arm cases and intend to present these in a future paper.

V. DISCUSSION AND RECONCILIATION

The final goal of producing noise curves and response functions is to answer the question of what gravitational wave sources are detectable. Several different approaches have been used in the literature to answer this question. It is the purpose of this section to discuss these different approaches and to try to reconcile them.

Section III discussed the actual strain noise spectral density [$S_n(f)$; see Fig. 2], and Sec. IV showed how the gravitational wave transfer function [$R(f)$; Fig. 4] is used to determine the gravitational wave sensitivity curve [$S_h(f)$; Fig. 5)]. The gravitational wave transfer function actually represents an averaged response of the interferometer, averaged over waves coming from different directions and having different wave polarizations. The transfer function, however, ignores the nature of the source creating the wave; no averaging was performed over parameters describing the sources themselves. Thus, the resulting gravitational wave sensitivity curve is equally appropriate for most types of sources. Of course, because of the averaging over direction, it is not completely appropriate for a source (like the interacting white dwarf binary AM *CVn*) whose direction is known. Nevertheless, this sensitivity curve seems to us to be a valuable intermediate tool to characterize the capability of gravitational wave detectors, especially since the strengths of the waves from many different types of sources may be plotted on this same graph. To calculate the gravitational-wave strength for a particular type of source as it is to be plotted on the sensitivity curve graph requires some additional steps specific to each class of sources.

A. Sensitivity to particular types of sources

For *continuous monochromatic sources* like circular compact binaries, the ultimate source sensitivity comes when the source is sampled for a long period of time so as to narrow the bandwidth, Δf. A continuous source with frequency f and amplitude h that is observed over a time T will appear in a Fourier spectrum of the data as a single spectral line with root spectral density

$$h_f = \frac{h}{\sqrt{\Delta f}} = h\sqrt{T}. \tag{48}$$

The frequency f and the amplitude h will depend on the several parameters of the binary such as total mass, semimajor axis, distance to the binary, inclination to the line-of-

sight, etc. If one wants to consider a population of monochromatic binaries, then an average over the parameters of possible systems should be taken, and the value used for h at each frequency should reflect this process.

For signals that are *short bursts*, such as would be produced by a compact body in highly elliptical orbit about a massive black hole or by high-velocity encounters of massive compact bodies in a region of high stellar density, the signal would typically have a characteristic pulse width τ with a broad spectral content and would occur only once in the lifetime of the detector. The detection of such a source is optimal when the bandwidth Δf is not much larger than τ^{-1}. The relationship between the amplitude of the pulse h and the strength of the signal as it would be plotted on the root spectral density graph is therefore given by

$$h_f = \frac{h}{\sqrt{\Delta f}} = h\sqrt{\tau}. \tag{49}$$

Again, if a population of burst sources is to be considered, then one should average the amplitudes over the possible parameters of the source, including all source orientations and accounting for the short duty cycles that such sources typically have.

Finally, one may consider how to include a *stochastic background* of gravitational waves as a source on the gravitational wave sensitivity graph. In some cases, such as the case of a stochastic superposition of close compact binary stars, the amplitude spectral density S_h is known. In these cases, the root spectral density

$$h_f(f) = \sqrt{S_h(f)} \tag{50}$$

can be plotted directly on the sensitivity graph. In other cases, what is assumed is a spectrum of the cosmic energy density, $\Omega(f)$. The relationship between amplitude and energy density is given by

$$S_h(f) = \frac{3H^2}{\pi^3 f^2}\Omega(f) \tag{51}$$

where H is the Hubble constant. The square root of $S_h(f)$ may again be plotted directly on the sensitivity graph. Finally, a cosmic background is often assumed to be simply peaked at some frequency, f_p, and spread over a decade of bandwidth. In this case, the bandwidth will be approximately equal to the peak frequency, and a point plotted at

$$h_f = \frac{3H}{\pi^{3/2} f_p^{3/2}}\Omega^{1/2} \tag{52}$$

would represent the peak of the decade-wide spectrum corresponding to a total integrated energy density of Ω.

B. Reconciliation with other results from the literature

Substantially different methods have often been used in the previous literature to illustrate the capability of a spaceborne interferometer to detect astrophysical sources of gravitational waves. This section describes how to relate the methods used in this work to the approach usually taken in the literature associated with the proposed LISA mission [3], and the comprehensive development of sensitivity limits provided in the review article of Thorne [14].

As in this paper, other analyses create an initial sensitivity curve for LISA by analyzing the various noise sources in the interferometer and then dividing by a transfer function [3,7]. The LISA instrumental sensitivity, in terms of h_f, is generally converted to an effective gravitational wave amplitude sensitivity, h, by dividing the value of h_f at each frequency by the square root of an assumed one year integration time. The resulting sensitivity curve in h is also multiplied by a factor of 5, so that the final curve indicates a one-year integrated threshold for a signal with signal-to-noise ratio $\geqslant 5$. The combination of these factors is

$$h_{\mathrm{SNR5}}^{1\mathrm{yr}} = 8.9\times 10^{-4} h_f, \tag{53}$$

where h_f is the spectral amplitude in units of $\mathrm{Hz}^{-1/2}$.

It should be emphasized that, after having assumed a one-year integration time, it is only appropriate to plot monochromatic gravitational wave sources against this type of sensitivity curve, and only for a case where a signal-to-noise ratio of 5 is actually required. The danger in using such a graph to characterize the overall detector sensitivity is that it is subject to easy misinterpretation, which has often occurred in the literature. An example is the paper by Aguiar *et al.* [12], which simply overestimates the LISA sensitivity to bursts from black hole oscillations lasting a few minutes by using the curves representing coherent integration of a signal for a year.[5] On the other hand, the usual LISA sensitivity curve graph underestimates LISA's sensitivity to monochromatic known sources, such as AM *CVn*, for which a signal-to-noise ratio of 5 is an excessive requirement.

Another approach is taken in the comprehensive review article by Thorne [14]. In this review, Thorne carefully distinguishes between the three types of source, and analyzes the response of a detector to each type. For each type of source, he finally derives a detector sensitivity which is denoted by $h_{3/yr}(f)$, defined as

$$h_{3/yr}(f) = 11[fS_h(f)]^{1/2} \quad \text{burst sources,} \tag{54}$$

$$h_{3/yr}(f) = 3.8[S_h(f)\times 10^{-7}\ \ \mathrm{Hz}]^{1/2} \quad \text{periodic sources,} \tag{55}$$

$$h_{3/yr}(f) = 4.5\left(\frac{\Delta f}{10^{-7}\ \ \mathrm{Hz}}\right)^{-1/4}[fS_h(f)]^{1/2}$$

$$\text{stochastic background.} \tag{56}$$

[5]The LISA team has recognized the difficulty of using such plots to characterize the detector sensitivity to bursts [13].

Here $S_h(f)$ is the same spectral density of detector noise utilized in this paper. The derived sensitivity, $h_{3/\mathrm{yr}}$, represents the weakest level at which one has 90% confidence of detecting a signal using two cross-correlated identical detectors. For burst sources, the level is set by demanding three detections per year. For periodic sources, $h_{3/\mathrm{yr}}$ represents the level obtained in a 1/3 year integration, assuming the frequency and phase of the source are known. Finally, for stochastic sources, $h_{3/\mathrm{yr}}$ represents the weakest source that can be detected with a 1/3 year integration of the cross-correlation function between two independent detectors.

The development of Thorne's three dicta for detection of burst, periodic, and stochastic sources involves detailed assumptions which are described at length in Ref. [14]; that discussion will not be reproduced in full here. It is worth noting, however, that not all of the assumptions made in the development of these dicta are valid for a space-based interferometer. For example, Thorne assumes one has two independent cross-correlated detectors. While this is a valid assumption for LIGO, it is not for a LISA-style instrument. Although the data from the three LISA arms can be treated as two interferometers, and hence measure both polarizations of gravitational waves, the two interferometers are not completely independent, as they share an arm.

VI. SUMMARY

Constructing the sensitivity curves for a spaceborne observatory, such as those shown in Fig. 5, is the first step in understanding the response of the instrument to gravitational radiation. The formalism developed here can be used to determine the sensitivity of *any* space-based interferometer simply in terms of the essential parameters which describe the overall design of the instrument. Not only does this allow one to quickly and accurately assess the performance of one proposed observatory compared to another, but it also provides a quick and easy method for considering new observatory designs.

Carefully detailing the response of any new instrument prepares us for the inevitable detection of unexplainable signals from distant astrophysical sources, and provides a clear idea of how to improve our instrumentation for the construction of the next generation of observatories.

ACKNOWLEDGMENTS

The work of S.L.L. and W.A.H. was supported in part by National Science Foundation Grant No. PHY-9734834 and NASA Cooperative Agreement No. NCC5-410.

[1] A. Ambramovici *et al.*, Science **256**, 325 (1992).
[2] C. Bradaschia *et al.*, Nucl. Instrum. Methods Phys. Res. A **289**, 518 (1990).
[3] P. Bender *et al.*, ''LISA Pre-Phase A Report'' (second edition) (1998).
[4] R. W. Hellings *et al.*, ''Orbiting Medium Explorer for Gravitational Astrophysics (OMEGA),'' proposal to NASA Medium Explorer program (1998) (unpublished).
[5] B. Warner, Astrophys. Space Sci. **225**, 249 (1995).
[6] J. W. Armstrong, F. B. Estabrook, and M. Tinto (unpublished).
[7] R. Schilling, Class. Quantum Grav. **14**, 1513 (1997).
[8] R. W. Hellings, in *The Detection of Gravitational Waves*, edited by D. G. Blair (Cambridge University Press, Cambridge, England, 1991), p. 453.
[9] F. B. Estabrook and H. D. Wahlquist, Gen. Relativ. Gravit. **6**, 439 (1975).
[10] M. Tinto and J. W. Armstrong, Phys. Rev. D **59**, 102003 (1999).
[11] G. Giampieri, Mon. Not. R. Astron. Soc. **289**, 185 (1997).
[12] O. D. Aguiar, J. C. N. de Araujo, M. T. Meliani, F. J. Jablonski, and M. E. Araujo, in *LASER INTERFEROMETER SPACE ANTENNA: Second International LISA Symposium*, edited by W. M. Folkner, AIP Conf. Proc. 456 (AIP, Woodbury, NY, 1998), p. 87.
[13] P. Bender *et al.*, ''LISA Pre-Phase A Report'' (Ref. [3]), p. 31.
[14] K. S. Thorne, in *300 Years of Gravitation*, edited by by S. W. Hawking and W. Israel (Cambridge University Press, Cambridge, England, 1987), pp. 330–438.